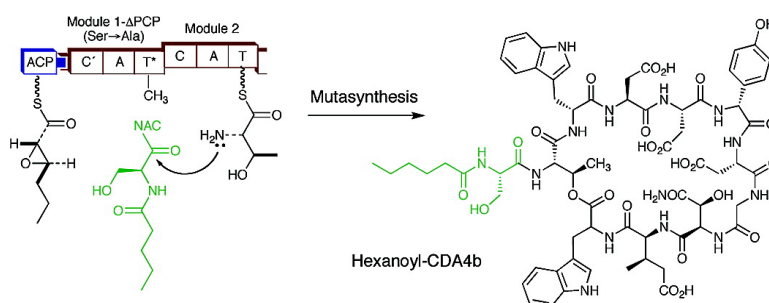


## Engineered Biosynthesis of Nonribosomal Lipopeptides with Modified Fatty Acid Side Chains

Amanda Powell, Mathew Borg, Bagher Amir-Heidari, Joanne M. Neary, Jenny Thirlway, Barrie Wilkinson, Colin P. Smith, and Jason Micklefield

*J. Am. Chem. Soc.*, **2007**, 129 (49), 15182-15191 • DOI: 10.1021/ja074331o

Downloaded from <http://pubs.acs.org> on February 9, 2009



### More About This Article

Additional resources and features associated with this article are available within the HTML version:

- Supporting Information
- Access to high resolution figures
- Links to articles and content related to this article
- Copyright permission to reproduce figures and/or text from this article

[View the Full Text HTML](#)

## Engineered Biosynthesis of Nonribosomal Lipopeptides with Modified Fatty Acid Side Chains

Amanda Powell,<sup>†</sup> Mathew Borg,<sup>‡</sup> Bagher Amir-Heidari,<sup>†,‡</sup> Joanne M. Neary,<sup>†,‡</sup> Jenny Thirlway,<sup>†</sup> Barrie Wilkinson,<sup>§</sup> Colin P. Smith,<sup>‡,○</sup> and Jason Micklefield<sup>\*,†,||</sup>

Contribution from the School of Chemistry and Department of Biomolecular Sciences, The University of Manchester, Oxford Road, Manchester M13 9PL, United Kingdom, and Biotica, Chesterford Research Park, Little Chesterford, Essex CB10 1XL, United Kingdom

Received June 14, 2007; E-mail: jason.micklefield@manchester.ac.uk

**Abstract:** The biological properties of the calcium-dependent antibiotics (CDAs), daptomycin and related nonribosomal lipopeptides, depend to a large extent on the nature of the *N*-terminal fatty acid moiety. It is suggested that the chain length of the unusually short (C6) 2,3-epoxyhexanoyl fatty acid moiety of CDA is determined by the specificity of the KAS-II enzyme encoded by *fabF3* in the CDA biosynthetic gene cluster. Indeed, deletion of the downstream gene *hxcO* results in three new lipopeptides, all of which possess hexanoyl side chains (hCDAs). This confirms that HxcO functions as a hexanoyl-CoA or -ACP oxidase. The absence of additional CDA products with longer fatty acid groups further suggests that the CDA lipid chain is biosynthesized on a single ACP and is then transferred directly from this ACP to the first CDA peptide synthetase (CdaPS1). Interestingly, the hexanoyl-containing CDAs retain antibiotic activity. To further modulate the biological properties of CDA by introducing alternative fatty acid groups, a mutasynthesis approach was developed. This involved mutating the key active site Ser residue of the CdaPS1, module 1 PCP domain to Ala, which prevents subsequent phosphopantetheinylation. In the absence of the natural module 1 PCP tethered intermediate, it is possible to effect incorporation of different *N*-acyl-L-serinyl *N*-acetylcysteamine (NAC) thioester analogues, leading to CDA products with pentanoyl as well as hexanoyl side chains.

### Introduction

The calcium-dependent antibiotics (CDAs, Figure 1A) from *Streptomyces coelicolor*<sup>1</sup> belong to the nonribosomally biosynthesized, acidic lipopeptide group of antimicrobial agents including the friulimicins,<sup>2</sup> A54145,<sup>3</sup> and daptomycin.<sup>4</sup> The acidic lipopeptides<sup>1–4</sup> coordinate calcium ions, which facilitate

aggregation and penetration into the cytoplasmic membranes of gram-positive bacteria.<sup>5</sup> This is postulated to generate pores in the membrane, which results in the loss of potassium ions, membrane depolarization, and ultimately cell death.<sup>5</sup> This group of antibiotics have become a major focus of attention since daptomycin became the first new structural class of natural antimicrobial agents to be approved for clinical use in over 30 years.<sup>4a,6</sup> Daptomycin is effective against gram positive pathogens, including methicillin and vancomycin resistant *Staphylococcus aureus*.<sup>4a,6</sup> However, resistance to daptomycin is particularly widespread in the environment,<sup>7</sup> increasing the probability that clinically relevant pathogens will acquire resistance through horizontal gene transfer.<sup>8</sup> It is thus highly

<sup>†</sup> School of Chemistry, The University of Manchester.  
<sup>‡</sup> Department of Biomolecular Sciences (ex-UMIST), The University of Manchester.  
<sup>§</sup> Biotica.  
<sup>||</sup> Present address: Manchester Interdisciplinary Biocentre, The University of Manchester, 131 Princess Street, Manchester M1 7DN, UK.  
<sup>⊥</sup> Present address: Pharmaceutical Technology Research Center, Kerman Medical University, Kerman, Iran.  
<sup>○</sup> Present address: Faculty of Health and Medical Sciences, University of Surrey, Guildford, GU2 7XH, U.K.

(1) (a) Hojati, Z.; Milne, C.; Harvey, B.; Gordon, L.; Borg, M.; Flett, F.; Wilkinson, B.; Sidebottom, P. J.; Rudd, B. A. M.; Hayes, M. A.; Smith, C. P.; Micklefield, J. *Chem. Biol.* **2002**, *9*, 1175–1187. (b) Kemper, C.; Kaiser, D.; Haag, S.; Nicholson, G.; Gnau, V.; Walk, T.; Gierling, G. H.; Decker, H.; Zahner, H.; Jung, G.; Metzger, J. W. *Angew. Chem., Int. Ed. Engl.* **1997**, *36*, 498–501. (c) Lakey, J. H.; Lea, E. J. A.; Rudd, B. A. M.; Wright, H. M.; Hopwood, D. A. *J. Gen. Microbiol.* **1983**, *129*, 3565–3573.  
(2) (a) Vértessy, L.; Ehlers, E.; Kogler, H.; Kurz, M.; Meiwes, J.; Seibert, G.; Vogel, M.; Hammann, P. *J. Antibiot.* **2000**, *53*, 816–827. (b) Heinzelmann, E.; Berger, S.; Müller, C.; Härtner, T.; Poralla, K.; Wohlleben, W.; Schwartz, D. *Microbiology* **2005**, *151*, 1963–1974.  
(3) (a) Fukuda, D. S.; Du Bus, R. H.; Baker, P. J.; Berry, D. M.; Mynderse, J. S. *J. Antibiot.* **1990**, *43*, 594–600. (b) Counter, F. T.; Allen, N. E.; Fukuda, D. S.; Hobbs, J. N.; Ott, J.; Ensminger, P. W.; Mynderse, J. S.; Preston, D. A.; Wu, C. Y. *J. Antibiot.* **1990**, *43*, 616–622. (c) Miao, V.; Brost, R.; Chapple, J.; She, K.; Coeffet-LeGal, M.-F.; Baltz, R. H. *J. Ind. Microbiol. Biotechnol.* **2006**, *33*, 66–74.

(4) (a) Baltz, R. H.; Miao, V.; Wrigley, S. K. *Nat. Prod. Rep.* **2005**, *22*, 717–741. (b) Miao, V.; Coeffet-LeGal, M.-F.; Brian, P.; Brost, R.; Penn, J.; Whiting, A.; Martin, S.; Ford, R.; Parr, I.; Bouchard, M.; Silva, C. J.; Wrigley, S. K.; Baltz, R. H. *Microbiology* **2005**, *151*, 507–523. (c) Debono, M.; Abbott, B. J.; Molloy, R. M.; Fukuda, D. S.; Hunt, A. H.; Daupert, V. M.; Counter, F. T.; Ott, J. L.; Carrell, C. B.; Howard, L. C.; Boeck, L. D.; Hamill, R. L. *J. Antibiot.* **1988**, *41*, 1093–1105.  
(5) (a) Straus, S. K.; Hancock, R. E. W. *Biochim. Biophys. Acta* **2006**, *1758*, 1215–1223. (b) Steenbergen, J. N.; Alder, J.; Thorne, G. M.; Tally, F. P. *J. Antimicrob. Chemother.* **2005**, *55*, 283–288. (c) Ball, L.-J.; Goult, C. M.; Donarski, J. A.; Micklefield, J.; Ramesh, V. *Org. Biomol. Chem.* **2004**, *2*, 1872–1878. (d) Micklefield, J. *Chem. Biol.* **2004**, *11*, 887–888. (e) Bunkoczi, G.; Vértessy, L.; Sheldrick, G. M. *Acta Crystallogr., Sect. D* **2005**, *61*, 1160–1164.  
(6) Raja, A.; LaBonte, J.; Lebbos, J.; Kirkpatrick, P. *Nat. Rev. Drug Discovery* **2003**, *2*, 943–944.  
(7) D'Costa, V. M.; McGrann, K. M.; Hughes, D. W.; Wright, G. D. *Science* **2006**, *311*, 374–377.

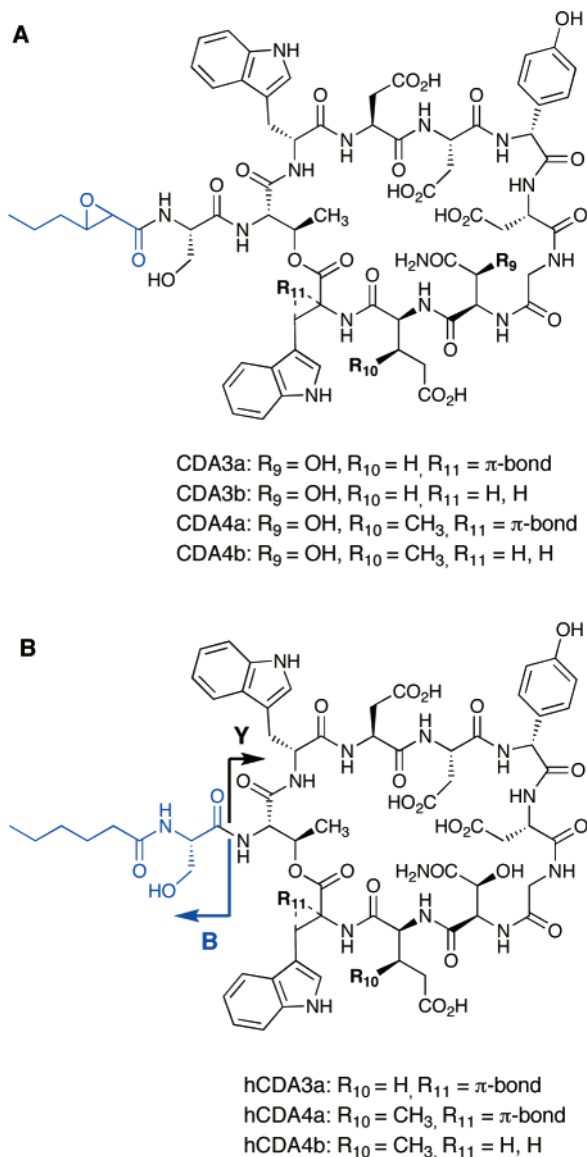


**Figure 1.** (A) The calcium-dependent antibiotics (CDAs) produced by the wild-type *S. coelicolor*. Other CDAs produced by the wild-type include CDA1b,  $R_9 = \text{OPO}_3\text{H}_2$ ,  $R_{10} = \text{H}$ ,  $R_{11} = \text{H,H}$ ; CDA2a,  $R_9 = \text{OPO}_3\text{H}_2$ ,  $R_{10} = \text{CH}_3$ ,  $R_{11} = \pi\text{-bond}$ ; CDA2b,  $R_9 = \text{OPO}_3\text{H}_2$ ,  $R_{10} = \text{CH}_3$ ,  $R_{11} = \text{H,H}$ . (B) Structures of hCDA4b, 4a, and 3a produced by the MT1110- $\Delta$ hxcO mutant strain. hCDA refers to hexanoyl-CDA, which is a variant of CDA that possesses a *N*-hexanoyl fatty acid side chain rather than the *N*-terminal *trans*-2,3-epoxyhexanoyl moiety found in the wild-type CDA.

desirable that future generations of acidic lipopeptides are developed to counter this.

The nature of the fatty acid groups of lipopeptides can dramatically affect both antimicrobial activity and toxicity in humans.<sup>3b,4a,c</sup> Furthermore, the lipopeptide fatty acid side chains are known to be susceptible to hydrolysis by deacylase enzymes of microbial origins.<sup>9</sup> Deacylation, along with other mechanisms that result in the loss of the essential lipid moieties from the peptide core, could prove to be just one of the ways in which lipopeptides are deactivated in the environment, as part of the

- (8) (a) Davies, J. *Science* **1994**, *264*, 375–382. (b) Weigel, L. M.; Clewell, D. B.; Gill, S. R.; Clark, N. C.; McDougal, L. K.; Flannagan, S. E.; Kolonay, J. F.; Shetty, J.; Killgore, G. E.; Tenover, F. C. *Science* **2003**, *302*, 1569–1571.  
 (9) (a) Takeshima, H.; Inokoshi, J.; Takada, Y.; Tanaka, H.; Omura, S. *J. Biochem.* **1989**, *105*, 606–610. (b) Boeck, L. D.; Fukuda, D. S.; Abbott, B. J.; Debono, M. *J. Antibiot.* **1988**, *41*, 1085–1092.

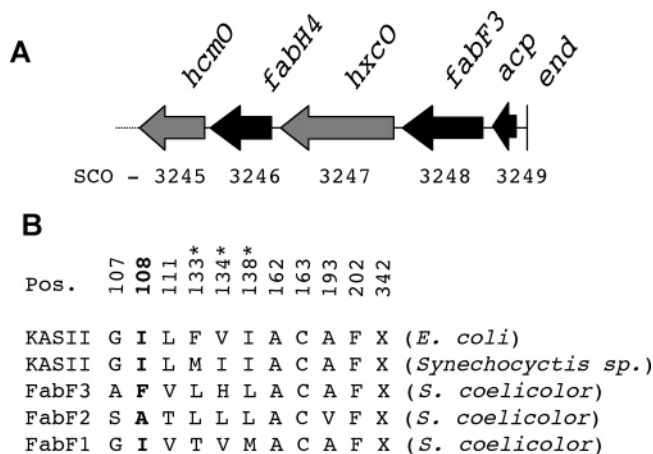


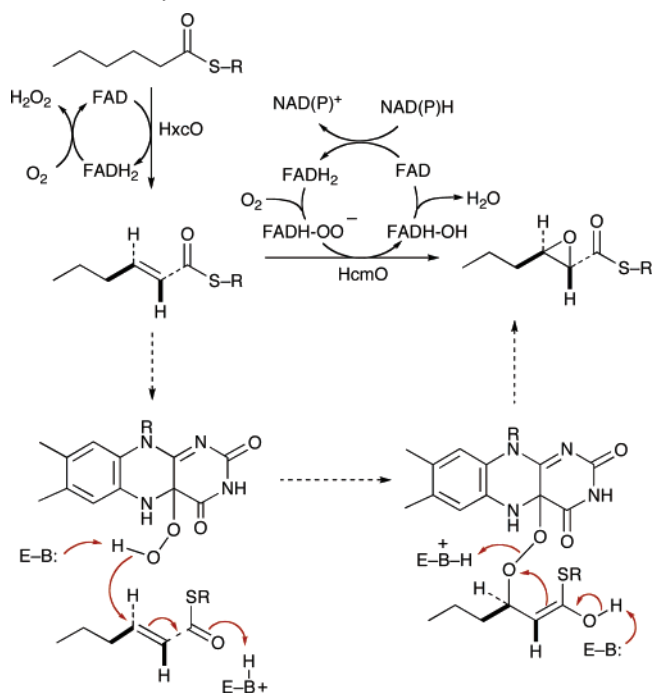
**Figure 2.** (A) The *fab* operon implicated in the biosynthesis of the CDA 2,3-epoxyhexanoyl fatty acid moiety. Each gene is labeled with the official SCO number (<http://streptomyces.org.uk/>). (B) Alignment of the known amino acid sequence of the acyl-substrate binding pockets of KAS-II enzymes from *E. coli* and *Synechocystis sp.*<sup>16</sup> with the putative substrate binding pockets of the KAS-II paralogs (FabF1–3) from *S. coelicolor*. The numbering system corresponds to the positions relative to the *E. coli* KAS-II enzyme. Residues indicated with an asterisk (\*) are known or assumed to come from a second protein subunit.<sup>16</sup>

microbial resistome.<sup>7</sup> In light of this, the development of new biosynthetic engineering approaches that allow for the replacement or modification of the fatty acid moieties of lipopeptides would be a logical step in the effort to generate new more potent and less toxic antimicrobial agents that might evade emerging resistance mechanisms. Several methods have been developed for engineering lipopeptides with different amino acid composition including: deletion of genes encoding amino acid biosynthesis and tailoring enzymes;<sup>10</sup> mutasynthesis;<sup>1a</sup> active site modification of adenylation (A)-domains;<sup>11</sup> and domain and module replacements within the nonribosomal peptide synthetase (NRPS) assembly line.<sup>12</sup> Despite this, there have been no general strategies available for engineering lipopeptides with modified fatty acid moieties. This is mainly due to the fact that little is known about the interplay between fatty acid and peptide assembly, in particular the mode by which the fatty acids are activated and then transferred to the NRPS prior to peptide assembly.

In the case of CDA, we identified a putative *fab* operon comprising 5 genes (SCO3245–SCO3249) situated at the end of the *cda* biosynthetic gene cluster (Figure 2A), which encode proteins that are predicted to be involved in the biosynthesis of the 2,3-epoxyhexanoyl fatty acid moiety of CDA.<sup>1a</sup> SCO3249 encodes a protein that is similar to acyl carrier proteins (ACPs) from fatty acid and polyketide synthases (FAS and PKS). SCO3248 (*fabF3*) and SCO3246 (*fabH4*) encode proteins that are similar to  $\beta$ -ketoacyl-ACP synthase KAS-II and -III

- (10) (a) Milne, C.; Powell, A.; Jim, J.; Al Nakeeb, M.; Smith, C. P.; Micklefield, J. *J. Am. Chem. Soc.* **2006**, *128*, 11250–11259. (b) Neary, J. M.; Powell, A.; Gordon, L.; Milne, C.; Flett, F.; Wilkinson, B.; Smith, C. P.; Micklefield, J. *Microbiology* **2007**, *153*, 768–776.  
 (11) (a) Uguru, G. C.; Milne, C.; Borg, M.; Flett, F.; Smith, C. P.; Micklefield, J. *J. Am. Chem. Soc.* **2004**, *126*, 5032–5033. (b) Eppelmann, K.; Stachelhaus, T.; Marahiel, M. A. *Biochemistry* **2002**, *41*, 9718–9726.  
 (12) (a) Stachelhaus, T.; Schneider, A.; Marahiel, M. A. *Science* **1995**, *269*, 69–72. (b) Mootz, H. D.; Kessler, N.; Linne, U.; Eppelmann, K.; Schwarzer, D.; Marahiel, M. A. *J. Am. Chem. Soc.* **2002**, *124*, 10980–10981. (c) Miao, V.; Coefflet-LeGal, M. F.; Nguyen, K.; Brian, P.; Penn, J.; Whiting, A.; Steele, J.; Kau, D.; Martin, S.; Ford, R.; Gibson, T.; Bouchard, M.; Wrigley, S. K.; Baltz, R. H. *Chem. Biol.* **2006**, *13*, 269–276. (d) Nguyen, K. T.; Ritz, D.; Gu, J.-Q.; Alexander, D.; Chu, M.; Miao, V.; Brian, P.; Baltz, R. H. *Proc. Natl. Acad. Sci. U.S.A.* **2006**, *103*, 17462–17467.

**Scheme 1.** Proposed Pathway and Mechanism for the Oxidation of the CDA Fatty Acid Side Chain<sup>a</sup>



<sup>a</sup> R = CoA or ACP. HxcO is putative hexanoyl-CoA or -ACP oxidase encoded by SCO3247, and HcmO is a putative *trans*-hexenoyl-CoA or -ACP mono-oxygenase encoded by SCO3245. Epoxidation, by a FAD-dependent mono-oxygenase, is most likely to involve the conjugate addition by the distal oxygen of flavin-C4a-hydroperoxide (FADH-OOH) to the electron-deficient double bond of the substrate to generate the enol-peroxyflavin intermediate, which can cyclize, eliminating flavin-C4a-hydroxide (FADH-OH).<sup>1a</sup> The absolute configuration of the *trans*-2,3-epoxyhexanoyl moiety is unknown and is shown arbitrarily as (2*S*,3*R*).

enzymes, respectively. KAS-III is required to initiate fatty acid synthesis, while KAS-II catalyzes subsequent condensation of saturated acyl-ACP intermediates with malonyl-CoA-derived precursors to generate longer fatty acids. The fourth gene of the *fab* operon, SCO3247, encodes a protein with highest similarity to FAD-dependent acyl-CoA oxidase enzymes and was tentatively assigned as a putative hexanoyl-CoA oxidase (HxcO) (Scheme 1).<sup>1a</sup> The final gene of the *cda fab* operon, SCO3245, encodes a protein that shows sequence similarity to *p*-hydroxybenzoate and salicylate hydroxylases<sup>13</sup> as well as zeaxanthin-epoxidase.<sup>14</sup> It is suggested that this enzyme may be responsible for the required epoxidation reaction following a mechanism that is similar to the cyclic ketone mono-oxygenases (Scheme 1).<sup>1a,15</sup>

## Results and Discussion

**KAS-II Sequence Alignments Reveal a Possible CDA Fatty Acid Chain Length Determinant.** The mixture of CDAs produced by *S. coelicolor* (Figure 1A) is unusual in that all variants have the same short 2,3-epoxyhexanoyl fatty acid side chain. All other acidic lipopeptides<sup>2–4</sup> belong to a family that possesses longer (>C10) fatty acid moieties, which differ significantly in their substitution patterns, degree of saturation, and chain length.<sup>4a</sup> To rationalize the origin of the unusually short C6 fatty acid side chain of CDA, the putative KAS-II

enzyme encoded by *fabF3* from within the *cda* cluster was aligned with the two other KAS-II paralogues from *S. coelicolor* and other bacterial KAS-II enzymes. This reveals a putative acyl-binding pocket similar to that of the KAS-II enzymes from *E. coli* and *Synechocystis* sp. whose structures have been elucidated by X-ray crystallography (Figure 2B).<sup>16</sup> However, while most of the other KAS-II enzymes have Ile at position 108 (*E. coli* numbering system), the *fabF3* encoded KAS-II of the *cda* cluster is distinct in possessing a Phe residue at the equivalent position. Interestingly, the X-ray crystal structures<sup>16</sup> show that Ile108 is in the middle of the hydrophobic acyl-substrate binding pocket. Moreover, mutation of the *E. coli* KAS-II, Ile108 residue to Phe abolishes the specificity for longer chain acyl-ACP (>C8) while retaining specificity for the shorter hexanoyl-ACP.<sup>16d</sup> It is thus likely that the Phe108 residue in KAS-II encoded by *fabF3* serves to reduce the size of the acyl-binding pocket, resulting in termination of fatty acid synthase (FAS) elongation at the hexanoyl-ACP intermediate.<sup>16d</sup>

**Deletion of the *hxcO* Gene.** To probe the biosynthetic origins of the CDA *trans*-2,3-epoxyhexanoyl fatty acid side chain, the *hxcO* gene was first deleted from the *S. coelicolor* genome using the double crossover recombination approach (see Supporting Information).<sup>17</sup> Thus, a 1887 bp DNA fragment incorporating 264 bp of the upstream end of *hxcO* and the adjacent SCO-3248 and -3249 (*fabF3* and *acp*) genes, and a fragment of 1689 bp including 333 bp of the downstream end of *hxcO* and the flanking SCO3246 (*fabH4*) gene, were PCR amplified. The fragments were then ligated into plasmid pMT3000, cloned, and then reisolated from *E. coli*. The resulting ca. 3.55 kb in-frame deletion fragment was digested from pMT3000 and sub-cloned into the plasmid pMAH,<sup>18</sup> which was used to transform protoplasts of *S. coelicolor* MT1110.<sup>19</sup> Subsequent homologous recombination and screening for second crossover recombination events<sup>1a,10</sup> resulted in the mutant strain  $\Delta hxcO$  (missing 1206 bp of *hxcO*). The successful generation of the required in-frame mutants was confirmed by Southern analysis and PCR amplification across the truncated region followed by DNA sequencing (see Supporting Information).

**Structure and Bioactivity of Hexanoyl CDAs.** The MT1110 parent and  $\Delta hxcO$  mutant strains were grown in liquid culture, and the culture supernatants were analyzed by LC-ESI-MS.<sup>1a,10</sup> This showed that the MT1110 parent strain produces CDA4a as the major product with a minor amount of CDA3a (see Supporting Information). The MT1110- $\Delta hxcO$  mutant, on the other hand, produces a new product with retention time 7.7 min, which exhibits a typical b-series CDA UV spectrum ( $\lambda_{\max}$  = 279 nm) and protonated, sodiated, and potassiated molecular ions in the ESI-MS, which correspond to mw 1482.3 (Figure 3). It transpires that this matches closely the mw of CDA3b; however, the retention time of an authentic sample of CDA3b was noticeably different (7.2 min) and does not coelute under the same HPLC conditions (see Supporting Information). To

(13) Ortiz-Maldonado, M.; Ballou, D. P.; Massey, V. *Biochemistry* **1999**, *38*, 8124–8137.

(14) Büch, K.; Stransky, H.; Hager, A. *FEBS Lett.* **1995**, *376*, 45–48.

(15) Sheng, D.; Ballou, D. P.; Massey, V. *Biochemistry* **2001**, *40*, 11156–11167.

(16) (a) Huang, W.; Joa, J.; Edwards, P.; Dehesh, K.; Schneider, G.; Lindqvist, Y. *EMBO J.* **1998**, *17*, 1183–1191. (b) Moche, M.; Schneider, G.; Edwards, P.; Dehesh, K.; Lindqvist, Y. *J. Biol. Chem.* **1999**, *274*, 6031–6034. (c) Moche, M.; Dehesh, K.; Edwards, P.; Lindqvist, Y. *J. Mol. Biol.* **2001**, *305*, 491–503. (d) Val, D.; Banu, G.; Seshadri, K.; Lindqvist, Y.; Dehesh, K. *Structure* **2000**, *8*, 565–566.

(17) Kieser, T.; Bibb, M. J.; Buttner, M. J.; Chater, K. F.; Hopwood, D. A. *Practical Streptomyces Genetics: A Laboratory Manual*; The John Innes Foundation: Norwich, UK, 2000.

(18) Bucca, G.; Brassington, A. M. E.; Hotchkiss, G.; Mersinias, V.; Smith, C. P. *Mol. Microbiol.* **2003**, *50*, 153–166.

(19) Hindle, Z.; Smith, C. P. *Mol. Microbiol.* **1994**, *12*, 737–745.



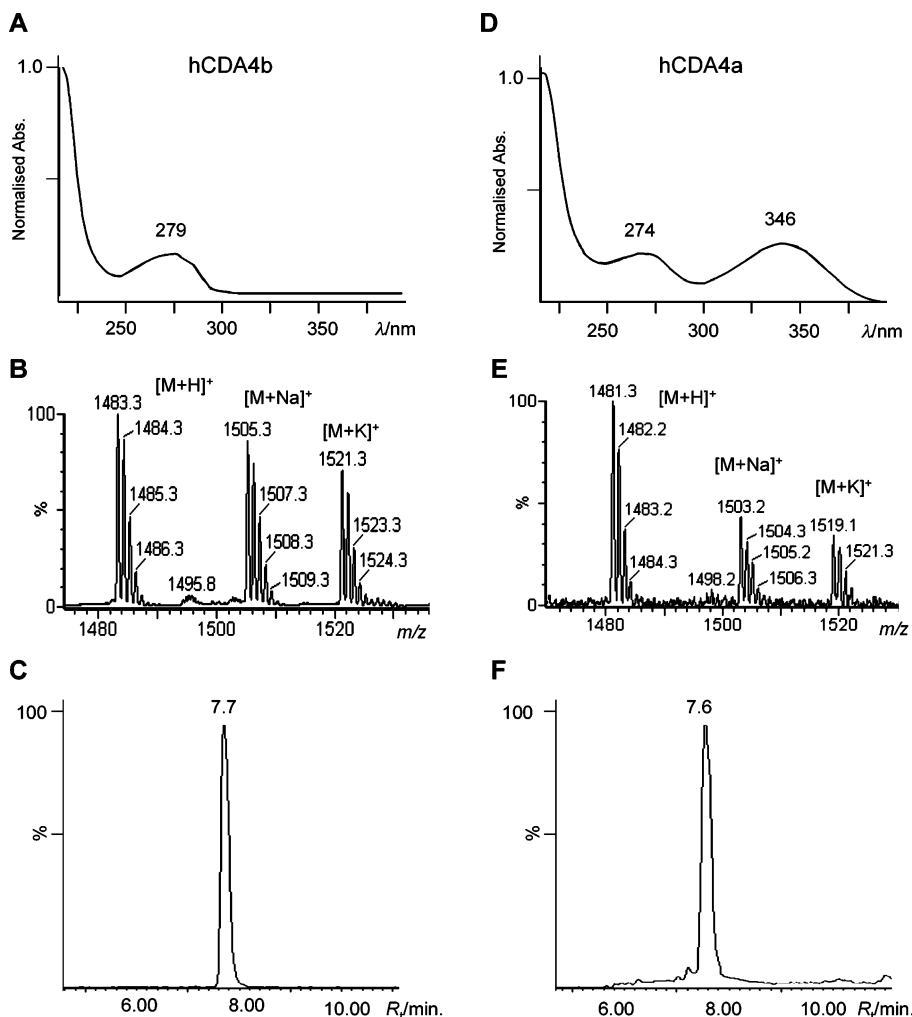


**Figure 3.** LC–MS and UV analysis of hCDA4b and hCDA4a isolated from MT1110- $\Delta$ hxcO grown on liquid and solid media, respectively: (A) UV spectrum of hCDA4b shows  $\lambda_{\max} = 279$  nm typical of the b-series CDA; (B) mass spectrum for hCDA4b is consistent with the proposed formula; (C) LC–MS chromatogram shows a retention time that is distinct from CDA3b, which shares the same molecular weight; (D) UV spectrum of hCDA4a shows  $\lambda_{\max} = 346$  nm typical of the Z-dehydrotryptophan-containing a-series CDA; (E) mass spectrum for hCDA4a is consistent with the proposed formula; and (F) LC–MS chromatogram shows a retention time that is distinct from CDA3a, which shares the same molecular weight.

**Table 1.** FT-ICR HRMS and MS–MS of hCDA4b and CDA4b<sup>a</sup>

ion	hCDA4b			CDA4b		
	formula	found	requires	formula	found	requires
[M + H] <sup>+</sup>	C <sub>67</sub> H <sub>83</sub> N <sub>14</sub> O <sub>25</sub> <sup>+</sup>	1483.5651	1483.5653	C <sub>67</sub> H <sub>81</sub> N <sub>14</sub> O <sub>26</sub> <sup>+</sup>	1497.5447	1497.5446
[M + 2H] <sup>2+</sup>	C <sub>67</sub> H <sub>84</sub> N <sub>14</sub> O <sub>25</sub> <sup>2+</sup>	742.2863	742.2866	C <sub>67</sub> H <sub>82</sub> N <sub>14</sub> O <sub>26</sub> <sup>2+</sup>	749.2825	749.2762
Y <sup>+</sup>	C <sub>58</sub> H <sub>68</sub> N <sub>13</sub> O <sub>22</sub> <sup>+</sup>	1298.4681	1298.4601	C <sub>58</sub> H <sub>68</sub> N <sub>13</sub> O <sub>22</sub> <sup>+</sup>	nd	1298.4601
[Y + H] <sup>2+</sup>	C <sub>58</sub> H <sub>69</sub> N <sub>13</sub> O <sub>22</sub> <sup>2+</sup>	649.7303	649.7340	C <sub>58</sub> H <sub>69</sub> N <sub>13</sub> O <sub>22</sub> <sup>2+</sup>	649.7281	649.7340
B <sup>+</sup>	C <sub>9</sub> H <sub>16</sub> NO <sub>3</sub> <sup>+</sup>	186.1112	186.1130	C <sub>9</sub> H <sub>14</sub> NO <sub>4</sub> <sup>+</sup>	200.0905	200.0923

<sup>a</sup> nd = not determined. Note that the HRMS and MS–MS data of hCDA4b clearly differ from those expected for the wild-type variant CDA3b ([M + H]<sup>+</sup> C<sub>66</sub>H<sub>79</sub>N<sub>14</sub>O<sub>26</sub>, requires 1483.5290; [M + 2H]<sup>2+</sup> C<sub>66</sub>H<sub>80</sub>N<sub>14</sub>O<sub>26</sub><sup>2+</sup>, requires 742.2684).

investigate the structure of this new CDA product, MT1110- $\Delta$ hxcO was cultivated on a larger scale and the CDA from the supernatant was purified by RP-HPLC. The new CDA was subjected to high-resolution MS on a 9.4 T FT-ICR instrument with an ESI source (Table 1). Both the singly charged [M + H]<sup>+</sup> and the doubly charged [M + 2H]<sup>2+</sup> molecular ions differ by ca. 25 ppm from the calculated value of CDA3b, but are within 0.5 ppm of the molecular formula of a CDA variant, which possesses a hexanoyl fatty side chain, hCDA4b (Figure 1B). To further confirm this structure, a tandem MS method was developed, which enabled the *trans*-2,3-epoxyhexanoyl-L-

Ser tail of CDAs to be fragmented from the decapeptide core. When this method was applied to the new CDA from MT1110- $\Delta$ hxcO, it was clearly apparent from the accurate masses of the B<sup>+</sup> and Y<sup>+</sup> ions, derived from the tail and core respectively (Figure 1B), that the new product has the same decapeptide core as CDA4b, but possesses a tail that is 14 mass units lower. The new product was therefore assigned as hexanoyl-CDA4b (hCDA4b).

During the HPLC purification of hCDA4b, the presence of a further peptide at low levels was evident. This exhibited a mw of 1480.5 Da, consistent with hCDA4a (the hexanoyl variant

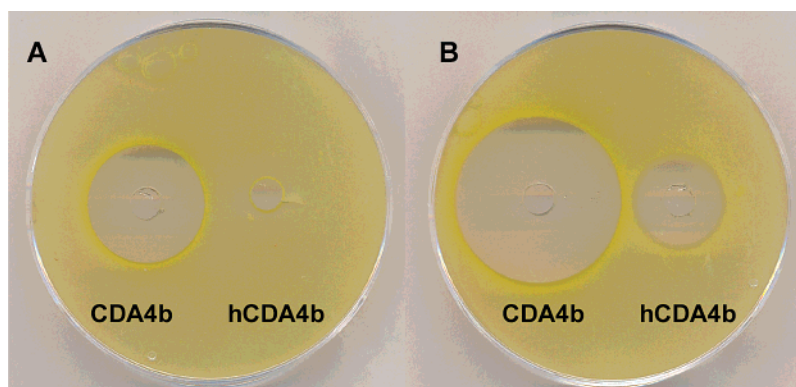


**Figure 4.** Bioassays of hCDA4b and the parent product CDA4b using *M. luteus* as the indicator strain in the presence of  $\text{Ca}^{2+}$  (16 mM).<sup>30</sup> (A) 10  $\mu\text{g}$  of CDA4b and hCDA4b in 100  $\mu\text{L}$  of deionized water (66.7  $\mu\text{M}$ ) were added to the 5 mm left- and right-hand wells, respectively. (B) As above except the concentration of CDA4b and hCDA4b is increased to 15  $\mu\text{g}$  in 100  $\mu\text{L}$  of deionized water (100  $\mu\text{M}$ ). Control experiments in the absence of  $\text{Ca}^{2+}$  show no zones of inhibition.

of CDA4a). This happens to be the same molecular weight as CDA3a, but once again the new product proved to have a retention time different from that of an authentic sample of CDA3a (see Supporting Information). To investigate its structure, the MT1110- $\Delta hxcO$  mutant was grown on solid media, which we have shown previously favors the production of the a-series, Z-dehydrotryptophan-containing, CDAs.<sup>1a</sup> As anticipated, growth under these conditions resulted in the hCDA4a variant as the major product. By pooling the exudates from large-scale solid media cultures, followed by repeated rounds of HPLC fractionation, it was possible to isolate a pure sample of hCDA4a. The UV spectrum of hCDA4a was typical of the a-series CDA ( $\lambda_{\text{max}} = 346 \text{ nm}$ ) (Figure 3), and high-resolution ESI-MS ( $m/z$  760.2620 [ $\text{M} + \text{K} + \text{H}$ ]<sup>2+</sup>,  $\text{C}_{67}\text{H}_{81}\text{N}_{14}\text{O}_{25}\text{K}^{2+}$  requires 760.2567) is consistent with proposed structure of hCDA4a (Figure 3). In addition, the MS-MS product ion spectrum resulting from the fragmentation of the hCDA4a doubly charged parent ion, obtained using an ESI-ion trap instrument, also reveals core fragments ( $\text{Y}^+$ ), which are consistent with hCDA4a (Figure 1B) possessing an hexanoyl fatty acid side chain (see Supporting Information). An additional product was also noted in the exudate from MT1110- $\Delta hxcO$  grown on solid media, which exhibited molecular ions, on LC-ESI-MS, which are consistent with hCDA3a.

Overall, these results are consistent with the gene product HxcO functioning as a hexanoyl-CoA or -ACP oxidase to give *trans*-hexenoyl-CoA or ACP prior to alkene epoxidation (Scheme 1). Presumably, deletion of the *hxcO* gene results in the accumulation of the hexanoyl precursor, which is transferred directly to the serinyl substrate tethered to the peptidyl carrier protein (PCP) domain of the first peptide synthetase (CdaPS1). In addition, purified samples of the hexanoyl containing CDAs (hCDA4a and hCDA4b) were subjected to well plate bioassays using *Micrococcus luteus* as an indicator strain, which confirmed that both products possess calcium-dependent antimicrobial activity. Comparison of the size of zones of inhibition from bioassay, using equimolar concentrations of hCDA4b and the parent CDA4b, indicates that hexanoyl-CDAs have lower antimicrobial activity than the 2,3-epoxyhexanoyl containing wild-type lipopeptides (Figure 4). Indeed, CDA4b shows a clear zone of calcium-dependent antibiosis at 13.3  $\mu\text{M}$  concentration, while hCDA4b does not exhibit antibiosis until ca. 100  $\mu\text{M}$ .

**Deletion of the *hcmO* Gene.** To further explore the biosynthesis of the CDA *trans*-2,3-epoxyhexanoyl side chain, the

putative mono-oxygenase encoding gene *hcmO* predicted to be responsible for the epoxidation step (Scheme 1) was deleted from the *S. coelicolor* MT1110 genome. This was achieved using the same double crossover recombination approach as described above. In this case, a 2.96 kb in-frame deletion construct (see Supporting Information) was generated using a DNA fragment of 1839 bp incorporating 177 bp of the upstream end of *hcmO* and the adjacent SCO3246 (*fabH4*) gene, and a fragment of 1101 bp including 177 bp of the downstream end of *hcmO* along with flanking gene SCO3244. The resulting mutant strain  $\Delta hcmO$  (missing 909 bp of *hcmO*) was shown to possess the required in-frame deletion by Southern analysis, PCR, and sequencing. LC-ESI-MS analysis of extracts from MT1110- $\Delta hcmO$  did not reveal any trace of CDA-like products within detection limits. Given that DNA sequencing of the truncated *hcmO* gene in the mutant strain ( $\Delta hcmO$ ) clearly shows that the gene deletion was in-frame, polar effects on downstream gene expression are unlikely to account for the loss of CDA production. Similarly, Southern analysis of  $\Delta hcmO$  (see Supporting Information) indicates that no genetic rearrangements have taken place. Therefore, the loss of CDA production is most likely due to the absence of the *hcmO* gene product.

While this indicates that HcmO is required for CDA biosynthesis, it does not provide any further insight into the specific function of the gene product. One possible explanation for this result is that a *trans*-hexenoyl-CoA or -ACP intermediate (Scheme 1) accumulates in the mutant, but is not recognized by the biosynthetic machinery that is responsible for fatty acid transfer to the NRPS. Alternatively, other enzymes of primary metabolism may transform the *trans*-hexenoyl-CoA or ACP intermediate.

**The Nature of Fatty Acid Precursors in CDA Biosynthesis.** Isolation of hexanoyl-CDAs from the MT1110- $\Delta hxcO$  mutant provides strong evidence for the role of HxcO in CDA biosynthesis. However, the exact nature of the substrates for HxcO and the putative mono-oxygenase HcmO is not clear. Previously, the similarity of HxcO to several acyl-CoA oxidases was used to argue that CDA fatty acid precursors were likely to exist as CoA-thioesters.<sup>1a</sup> To explore this possibility, HxcO was overproduced in *E. coli* BL21 (DE3) as a his<sub>6</sub>-tag fusion protein using the pET-15b (Novagen) expression vector, induced by addition of IPTG. Purification by nickel chelate chromatography under native conditions gave a protein, which by SDS-PAGE and Western blots was consistent with the calculated

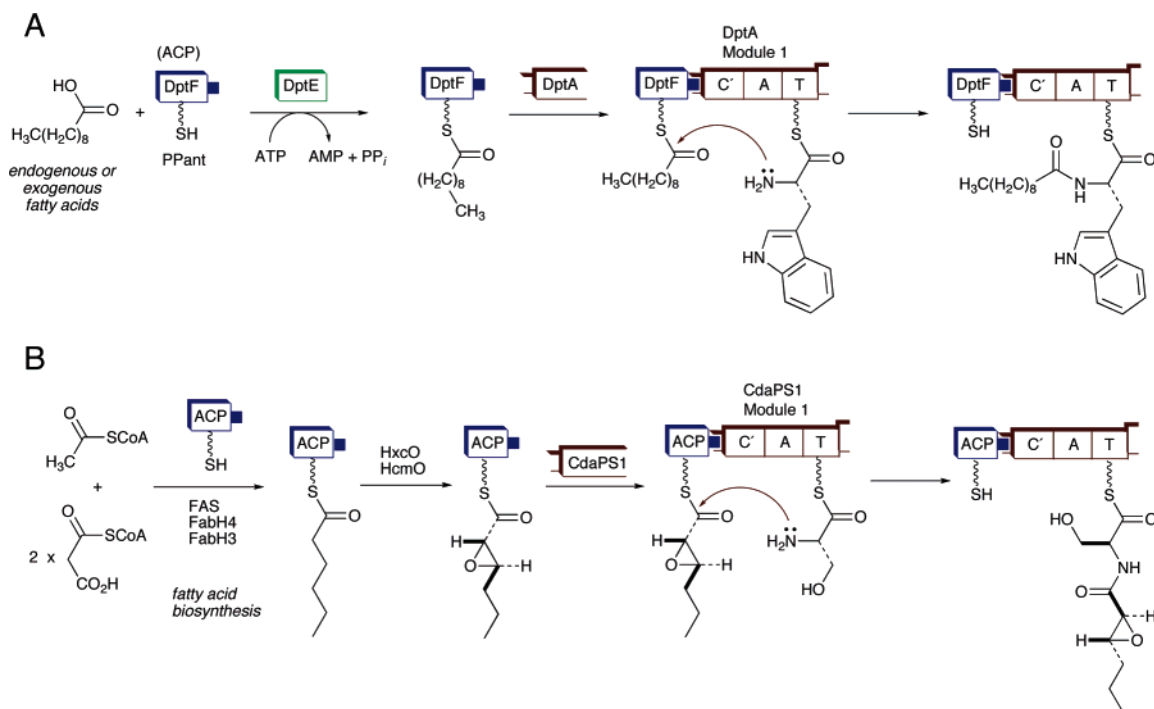


**Figure 5.** (A) Proposed mode of fatty acid activation and transfer in daptomycin biosynthesis. DptE is a putative adenylating enzyme, and DptF is a stand-alone ACP.<sup>4b</sup> In A54145 biosynthesis, a single protein, LptEF,<sup>3c</sup> is predicted to carry out the same function. The N-terminal C'-domains of nonribosomal lipopeptide synthetase enzymes share significant sequence similarity, but differ from standard NRPS C-domains within elongation modules. (B) Proposed mode of fatty acid assembly and transfer during CDA biosynthesis, with a single ACP predicted to be involved in both fatty acid biosynthesis, and subsequent oxidation and transfer of the 2,3-epoxyhexanoyl moiety. The fact that the C'-domains of DptA and CdaPS1 exhibit sequence similarity suggests a similar mechanism of fatty acid transfer and initiation of lipopeptide assembly.

mw of the putative HxcO (64.0 kDa) (see Supporting Information). The recombinant HxcO protein was then subjected to a series of typical assays for acyl-CoA oxidase and acyl-CoA dehydrogenase activity, in the presence of the putative hexanoyl-CoA substrate. However, under the conditions that were investigated, there was no apparent oxidation of hexanoyl-CoA. One reason for this could be the possibility that hexanoyl-ACP, rather than the hexanoyl-CoA, is the substrate for HxcO.

In the case of daptomycin,<sup>4b</sup> A54145,<sup>3c</sup> the friulimicins,<sup>2b</sup> and related lipopeptides, it is postulated<sup>20</sup> that an adenylating enzyme, with similarity to acyl-CoA synthetase, activates endogenous fatty acids as acyl-AMP intermediates, which are then transferred to the phosphopantetheine cofactor of an ACP, in a fashion functionally similar to that of the acyl-AMP ligases from mycobacteria.<sup>20,21</sup> It is then predicted that the fatty acid chain is transferred from the ACP to the NRPS in a reaction mediated by the N-terminal condensation (C') domain (Figure 5A). The fact that daptomycin, A54145, and the friulimicins are produced as a mixture containing a diverse range of lipid chains indicates that this mode of fatty acid activation and transfer is promiscuous and is likely to be primarily governed by protein:protein interactions between the ACP and C'-domain (Figure 5A). Interestingly, homologues of DptE and DptF are not present in the CDA biosynthetic cluster, suggesting that biosynthesis and/or activation of the CDA *trans*-2,3-epoxyhexanoyl-fatty acid side chain occurs by a distinct pathway. Indeed, the results presented here and elsewhere<sup>1a</sup> are consistent with a

pathway that is mediated by a single ACP encoded by SCO3249 (Figure 5B). In this pathway, hexanoyl-ACP is produced by *fabF3* and *fabH4* encoded KAS II and III, in combination with primary metabolic FAS components. It is then postulated that the hexanoyl substrate tethered to the same ACP undergoes subsequent desaturation and epoxidation reactions catalyzed by HxcO and HcmO, respectively. Finally, the 2,3-epoxyhexanoyl moiety is transferred from the ACP to the first amino acid, Ser, tethered to the module 1 PCP of CdaPS1, in a reaction potentially catalyzed by the N-terminal condensation (C') domain (Figure 5B).

**Mutasynthesis<sup>22</sup> of CDAs with Modified Fatty Acid Side Chains.** In daptomycin biosynthesis, it is possible to change the nature of the fatty acid moiety by feeding alternative fatty acids to the producer strain.<sup>4,23</sup> In the case of CDA, similar precursor-directed biosynthesis approaches do not result in modified lipopeptides. Presumably, this is due to differences in the mode of fatty acid activation prior to transfer onto the NRPS (Figure 5). In light of this, we sought to develop a mutasynthesis<sup>22</sup> approach, which would circumvent the fatty acid loading step and allow the direct incorporation of synthetic *N*-acyl-L-serinyl precursors as *N*-acetylcysteamine (NAC) thioester analogues of the first intermediate generated by module 1 of CdaPS1 (Figure 6). Cell-permeable NAC thioester analogues of polyketide intermediates have been successfully incorporated

(20) Grünewald, J.; Marahiel, M. A. *Microbiol. Mol. Biol. Rev.* **2006**, *70*, 121–146.

(21) Trivedi, O. A.; Arora, P.; Sridharan, V.; Tickoo, R.; Mohanty, D.; Gokhale, R. S. *Nature* **2004**, *428*, 441–445.

(22) Mutasynthesis generally involves blocking a biosynthetic pathway by deleting a specific gene encoding an enzyme on the pathway. The resulting mutant, which is unable to produce downstream intermediates and products, is then fed an analogue of one of the intermediates, which can be incorporated into the pathway leading to the biosynthesis of a natural product analogue with modified functionality.

(23) Huber, F. M.; Pieper, R. L.; Tietz, A. J. *J. Biotechnol.* **1988**, *7*, 283–292.

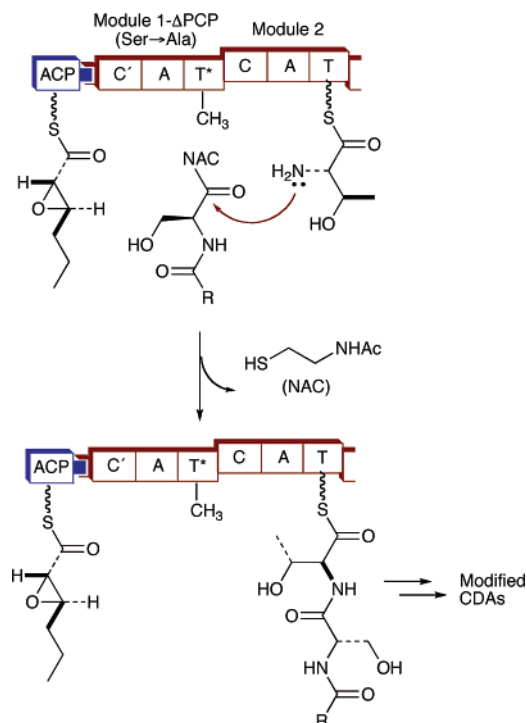
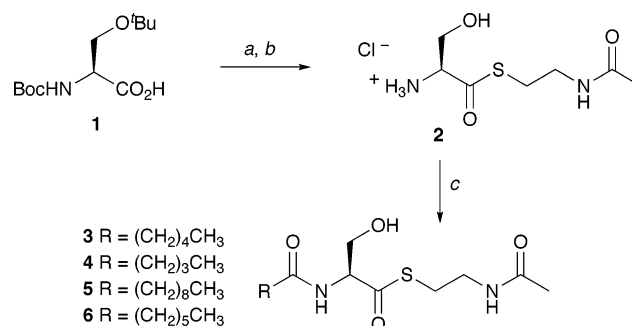


**Figure 6.** Mutasynthesis of CDA with modified fatty acid side chains. Site-directed mutagenesis of the module 1 PCP domain, changing the active site Ser to Ala, results in a mutant MT1110- $\Delta$ PCP1, which lacks the essential phosphopantetheine prosthetic group. As a result of this, the 2,3-epoxyhexanoyl precursor tethered to the upstream ACP cannot be transferred to the mutant PCP domain of module 1, and production of wild-type CDA is abolished. In the absence of the natural 2,3-epoxyhexanoyl-L-serinyl intermediate, on module 1, exogenous supply of the *N* $\alpha$ -hexanoyl and *N* $\alpha$ -pentanoyl-L-serinyl *N*-acetylcysteamine thioester **3** and **4** results in the production of hexanoyl- and pentanoyl-CDAs.

into polyketide products by PKS enzymes *in vivo*.<sup>24</sup> However, as far as we are aware, this approach has not been employed for the precursor-directed biosynthesis of nonribosomal peptides. Nevertheless, *in vitro* studies have demonstrated that amino acyl- and peptidyl-NAC thioesters function as substrates for both condensation and thioesterase domains within NRPS enzymes.<sup>25</sup> However, if this approach is to be successful *in vivo*, it is probably desirable to alleviate competition with the natural substrates.<sup>24a</sup> To this end, we chose to mutate the key active site Ser residue of the module 1 PCP domain to an Ala residue. This single point mutation is not likely to affect the overall conformation of the NRPS, but will prevent phosphopantetheinylation of the PCP domain and abolish CDA production. In the absence of the *N*-epoxyhexanoyl-L-serinyl-S-PCP intermediate on module 1, it should then be possible for exogenous, synthetic *N*-acyl-L-serinyl-NAC analogues to function as substrates for the downstream condensation domain,<sup>25a,b</sup> thereby reinitiating biosynthesis of CDAs.

To explore this mutasynthesis approach, a 1.52 kb DNA fragment encompassing the module 1 PCP-domain was derived by PCR from *cdaPS1*, ligated into plasmid pGEM11Zf(+) (Stratagene), cloned, and then reisolated from *E. coli*. The

**Scheme 2.** Synthesis of *N* $\alpha$ -Acyl-L-serine *N*-Acetylcysteamine Thioester **3**–**6**<sup>a</sup>



<sup>a</sup> Conditions: (a) DCC, HOBT, AcNH(CH<sub>2</sub>)<sub>2</sub>SH, THF; (b) 4 M HCl in dioxane; (c) pentanoyl, hexanoyl, or heptanoyl chloride, Et<sub>3</sub>N, CH<sub>2</sub>Cl<sub>2</sub>, -78 °C (for **5**, decanoyl *N*-hydroxysuccinimide ester, THF, Et<sub>3</sub>N, room temperature).

resulting plasmid was then mutated using the QuikChange method (Stratagene) to generate a plasmid coding for a Ser1122→Ala single-point mutant. The 1.52 kb DNA fragment containing the point mutation was then sub-cloned into the plasmid pMAH,<sup>18</sup> which was used to transform protoplasts of *S. coelicolor* MT1110.<sup>19</sup> Subsequent screening of second cross-over recombination events resulted in MT1110- $\Delta$ *pcp1* mutants, which were confirmed by sequencing of genomic DNA to possess the required codon change (Ser1122→Ala). The MT1110- $\Delta$ *pcp1* mutants were then grown in liquid culture, and the supernatants were analyzed by LC–MS. This revealed the complete absence, within detection limits, of any wild-type CDAs. In addition, both cell-based and well-based bioassays revealed that MT1110- $\Delta$ *pcp1* extracts fail to show calcium-dependent anti-biosis typical of the extracts from the parental strain.

With the mutant in hand, *N*-hexanoyl- and *N*-pentanoyl-L-serinyl NAC thioesters **3** and **4** were synthesized (Scheme 2) from protected serine derivative **1**, via the L-serinyl NAC thioester **2**.<sup>24a</sup> The NAC thioesters **3** and **4** were then fed at different concentrations ranging from 0.1 to 4.0 mg mL<sup>-1</sup> to the MT1110- $\Delta$ *pcp1* strain grown in liquid culture. In the case of *N*-hexanoyl-L-serinyl NAC thioester **3**, feeding above 1.7 mg mL<sup>-1</sup> to MT1110- $\Delta$ *pcp1* results in production of a product with identical retention time and protonated, sodiated, and potassiated singly and doubly charged molecular ions in the ESI-MS, as the hCDA4b that was isolated from MT1110- $\Delta$ *hxcO*. Production levels of hCDA4b in these experiments were, however, low, even at high concentrations of **3** (4.0 mg mL<sup>-1</sup>), as compared to levels of hCDA4b obtained from the MT1110- $\Delta$ *hxcO* mutant. This may be due to the instability of **3** *in vivo*, which is likely to be susceptible to hydrolysis by nonspecific protease and lipase enzymes over the 4 days of fermentation. Nevertheless, it is clear that production of hCDA4b in MT1110- $\Delta$ *pcp1* is entirely dependent on the presence of *N*-hexanoyl-L-serinyl NAC thioesters **3**. Furthermore, feeding experiments with the *N*-pentanoyl-L-serinyl NAC thioester **4** and MT1110- $\Delta$ *pcp1* resulted in a new product of lower retention time, which exhibits singly and doubly charged molecular ions that are consistent with a pentanoyl lipopeptide variant (pCDA4b). Once again, this new product is produced at low levels in the presence of **4** and is clearly not evident in control fermentations in the absence of **4**.

In the case of daptomycin, it was previously established that the lipopeptide with a decanoyl fatty acid moiety showed

(24) (a) Jacobsen, J. R.; Hutchinson, C. R.; Cane, D. E.; Khosla, C. *Science* **1997**, *277*, 367–369. (b) Boddy, C. N.; Hotta, K.; Tse, M. L.; Watts, R. E.; Khosla, C. *J. Am. Chem. Soc.* **2004**, *126*, 7436–7437.  
(25) (a) Ehmman, D. E.; Trauger, J. W.; Stachelhaus, T.; Walsh, C. T. *Chem. Biol.* **2000**, *7*, 765–772. (b) Roche, E. D.; Walsh, C. T. *Biochemistry* **2003**, *42*, 1334–1344. (c) Trauger, J. W.; Kohli, R. M.; Mootz, H. D.; Marahiel, M. A.; Walsh, C. T. *Nature* **2000**, *407*, 215–218.



optimum biological activity.<sup>4</sup> To explore if the mutasynthesis approach developed here could be used to prepare decanoyl CDA variants, the *N*-decanoyl-L-serinyl NAC thioester **5** was prepared. When **5** was fed to MT1110- $\Delta$ *pcp*<sub>1</sub> at concentrations up to 4.0 mg mL<sup>-1</sup>, cell growth was maintained, but there was no decanoyl CDA production evident in the culture supernatants at the LC-MS detection threshold. When feeding higher concentrations of **5** (above 4.0 mg mL<sup>-1</sup>), significant inhibition of cell growth was observed. This is most likely due to hydrolysis of **5** releasing decanoic acid, which is known to be highly toxic to streptomycetes causing cell lysis.<sup>23</sup> Indeed, the production of daptomycin by feeding decanoic acid to the producer strain *S. roseosporus* is only possible using large-scale fermentors (+120 L), which allow the continuous infusion of decanoic acid into the culture medium.<sup>23</sup> Such fermentation technology was not available for this study, and so this approach was not explored. However, to further investigate the effects of fatty acid chain length, the heptanoyl-L-serinyl NAC thioester **6** was fed to MT1110- $\Delta$ *pcp*<sub>1</sub>. While the heptanoyl variant did not affect the growth of the mutant strain, it did not result in production of CDAs containing heptanoyl side chains. Therefore, in addition to the postulated specificity of the KAS-II enzyme, encoded by *fabF3*, it appears that the CDA NRPS also possesses specificity for substrates with C6 or shorter *N*-acyl groups. Most likely, this specificity would operate within the first condensation domain, which catalyzes the peptide bond-forming reaction between the *N*-acyl-L-serinyl NAC thioesters and the Thr residue tethered to the module 2 PCP domain (Figure 6). In addition, it is also known from in vitro biochemical studies that the efficient regioselective cyclization of CDA linear undecapeptides by the CDA TE domain (cyclase) is dependent upon the nature of the *N*-acyl substituent, with the C6 *N*-acyl group favoring regioselective cyclization over hydrolysis.<sup>26a</sup> However, it is also noted that the CDA TE was shown to catalyze cyclization of linear daptomycin peptide precursors (13 mer), with C10 *N*-acyl side chains, albeit with increased hydrolysis side products.<sup>26b</sup> Thus, while the TE domain may demonstrate some selectivity toward the CDA precursors with C6 *N*-acyl groups, it is unlikely to be the main specificity determinant.

If one also considers that CDAs are atypical in that all natural variants possess the same C6-fatty acid side chain, while all other lipopeptides are produced with a wide variety of different lipid groups, then the results presented here are not necessarily surprising. Clearly, the biosynthesis of CDA has evolved to conserve the C6-fatty acid moiety. Moreover, this would most likely be achieved by restricting the size of the hydrophobic pockets of the active sites that bind the acyl group on both the FAS and the NRPS assembly lines.

This mutasynthesis approach is significant because it demonstrates, for the first time, how amino acyl-NAC thioester analogues can be used to probe substrate specificity of NRPSs in vivo, as well as enabling precursor directed biosynthesis of “unnatural” nonribosomal peptides. The fact that the yield and range of substrates that can be introduced into CDA are limited can be considered as a consequence of the typically low titers observed for lipopeptide production in *S. coelicolor*, combined with the apparent tight specificity of the CDA NRPS assembly

line. However, application of this mutasynthesis approach with industrial lipopeptide-producing strains, such as *S. roseosporus*, would no doubt be much more powerful. Not only do such strains produce lipopeptides with a wide variety of lipid groups, indicating relaxed specificity of the assembly line enzymes, but production levels under optimized fermentation conditions are several orders of magnitude higher than for *S. coelicolor*.<sup>27</sup> This could allow the production of sufficient quantities of “unnatural” lipopeptides for biological evaluation.

## Conclusions

CDAs are unusual among lipopeptides, as they all possess short (C6) 2,3-epoxyhexanoyl fatty acid side chains. Sequence alignment of a putative KAS-II enzyme, encoded by *fabF3* within the *cda* cluster, reveals an atypical active site Phe residue, which is predicted to block the substrate acyl binding pocket, thereby preventing extension beyond the (C6) hexanoyl precursor.<sup>16</sup> Deletion of the downstream *hxcO* gene results in the production of three new products, all possessing hexanoyl fatty acid side chains (hCDAs). This confirms the involvement of HxcO in the oxidation of a hexanoyl precursor prior to epoxidation and represents one of the first examples of rational biosynthetic engineering leading to new nonribosomal lipopeptides with modified fatty acid side chains. The fact that the hexanoyl precursor is able to initiate lipopeptide biosynthesis also indicates that fatty acid transfer to the substrate Ser on the NRPS (CdaPS1) is not specific for the 2,3-epoxyhexanoyl group. Indeed, it is suggested that the CDA fatty acid moiety is first synthesized on an ACP (encoded by SCO3249), oxidized by HxcO and HcmO, and then transferred from the same ACP to CdaPS1. This contrasts with the biosynthesis of other lipopeptides, where activation and transfer of a wide range of endogenous and exogenously supplied fatty acids occurs. In addition to this, a mutasynthesis strategy was developed that enables the directed biosynthesis of CDAs with alternative fatty acid moieties. This approach relies on the key Ser→Ala point mutation in the module 1 PCP domain of CdaPS1, which prevents phosphopantetheinylation and subsequent accumulation of the *N*-epoxyhexanoyl-L-serinyl-S-PCP intermediate, allowing incorporation of exogenously supplied synthetic *N*-acyl-L-serinyl-NAC analogues. This is important given that the epoxide moiety of the CDA lipid chain is not essential for antibiotic activity of CDAs. Indeed, the availability of new methods to modify the nature of the lipid moiety may prove useful in modulating the biological properties of clinically relevant lipopeptide antibiotics to counter the emerging threat of pathogens acquiring resistance from the environment.<sup>7,8</sup>

## Experimental Section

**L-Serine *N*-Acetylcysteamine Thioester Hydrochloride (2).** *N*-Boc-*O*-*t*-Bu-L-serine *N*-acetylcysteamine thioester (2.5 g) was prepared as described previously<sup>25a</sup> and treated with 4 M HCl in 1,4-dioxane (10 mL) at 0 °C. After being stirred for 10 min, the mixture was allowed to warm to room temperature with stirring for 3 h. The solvent was evaporated under reduced pressure. Recrystallization of the solid residue from CH<sub>3</sub>OH/CH<sub>2</sub>Cl<sub>2</sub> gave the product **2** (1.32 g, 79%) as a white solid: *R*<sub>f</sub> = 0.4 (20% H<sub>2</sub>O in CH<sub>3</sub>CN); mp 80–81 °C; <sup>1</sup>H NMR (400

(26) (a) Grünewald, J.; Sieber, S. A.; Marahiel, M. A. *Biochemistry* **2004**, *43*, 2915–2925. (b) Grünewald, J.; Sieber, S. A.; Mahlert, C.; Linne, U.; Marahiel, M. A. *J. Am. Chem. Soc.* **2004**, *126*, 17025–17031.

(27) The production levels of the wild-type CDAs in the parental *S. coelicolor* MT1110 or 2377 strains are typically modest (ca. 10 mg L<sup>-1</sup>). However, daptomycin and related lipopeptides are produced in *Streptomyces roseosporus*, under optimized fermentation conditions with titres of ca. 1000 mg L<sup>-1</sup> (see refs 4 and 23).

MHz, DMSO-*d*<sub>6</sub>) δ 1.80 (3H, s, COCH<sub>3</sub>), 3.00–3.05 (2H, m, SCH<sub>2</sub>), 3.22 (2H, q, *J* = 6.5 Hz, NHCH<sub>2</sub>), 3.86 (2H, d, m, CH<sub>2</sub>OH), 4.33 (1H, t, *J* = 3.5 Hz, CHCH<sub>2</sub>), 5.67 (1H, brs, OH), 8.20 (1H, m, NHCH<sub>2</sub>), 8.53 (3H, brs, NH<sub>3</sub><sup>+</sup>); <sup>13</sup>C NMR (100.6 MHz, DMSO-*d*<sub>6</sub>) δ 22.9 (COCH<sub>3</sub>), 28.7 (SCH<sub>2</sub>), 38.2 (NHCH<sub>2</sub>), 60.8 (CH<sub>2</sub>CH), 61.1 (CHCH<sub>2</sub>), 169.8 (COCH<sub>3</sub>), 195.1 (CHCOS); LRMS-ESI (*m/z*) 207.1 ([M – Cl]<sup>+</sup>, 100%); HRMS-ESI (*m/z*) [M – Cl]<sup>+</sup> calcd for C<sub>7</sub>H<sub>15</sub>N<sub>2</sub>O<sub>3</sub>S, 207.0803. Found, 207.0803. Anal. Calcd for C<sub>7</sub>H<sub>15</sub>N<sub>2</sub>O<sub>3</sub>SCl: C, 34.6; H, 6.2; Cl, 14.6; N, 11.5; S, 13.2. Found: C, 34.4; H, 6.1; Cl, 15.0; N, 11.3; S, 12.9. [α]<sub>D</sub> = +25.8° (*c* = 0.5, MeOH).

**Nα-Hexanoyl-L-serine N-Acetylcysteamine Thioester (3).** To L-Ser-NAC·HCl **2** (260 mg, 1.1 mmol) in dry CH<sub>2</sub>Cl<sub>2</sub> (5 mL), under N<sub>2</sub>, was added Et<sub>3</sub>N (298 μL, 2.14 mmol). The mixture was stirred at room temperature for 5 min and cooled to –78 °C, under N<sub>2</sub>. Hexanoyl chloride (147 μL, 1.05 mmol) was added dropwise with stirring over 5 min. After further stirring for 30 min at –78 °C, another portion of Et<sub>3</sub>N (75 μL, 54 mmol) was added followed by hexanoyl chloride (32 μL, 0.23 mmol). The mixture was stirred at –78 °C for 20 min and then was allowed to warm to room temperature. Water (20 mL) was added, and the mixture was extracted with CH<sub>2</sub>Cl<sub>2</sub> (3 × 5 mL). The organic extracts were dried over MgSO<sub>4</sub>, evaporated under reduced pressure, and purified by column chromatography over silica gel eluting with 0→10% CH<sub>3</sub>OH in EtOAc to afford the product **3** (255 mg, 78%) as a clear oil. *R*<sub>f</sub> 0.25 (10% CH<sub>3</sub>OH in ethyl acetate); <sup>1</sup>H NMR (400 MHz, CDCl<sub>3</sub>) 0.90 (3H, t, *J* = 6.9 Hz, CH<sub>3</sub>CH<sub>2</sub>), 1.31 (4H, m, CH<sub>3</sub>CH<sub>2</sub>CH<sub>2</sub>), 1.65 (2H, m, CH<sub>2</sub>CH<sub>2</sub>CO), 1.94 (3H, s, CH<sub>3</sub>CO), 2.28 (2H, t, *J* = 7.5 Hz, CH<sub>2</sub>CH<sub>2</sub>CO), 2.92–3.05 (2H, m, SCH<sub>2</sub>), 3.34–3.47 (2H, m, NHCH<sub>2</sub>), 3.75 (1H, dd, *J* = 3.2, 11.5 Hz, CHCH<sub>a</sub>H<sub>b</sub>O), 4.08 (1H, dd, *J* = 2.7, 11.5 Hz, CHCH<sub>a</sub>H<sub>b</sub>O), 4.59–4.61 (1H, m, CHCH<sub>2</sub>), 6.78 (1H, brs, CH<sub>2</sub>NHCO), 7.14 (1H, d, *J* = 7.8 Hz, CHNHCO); <sup>13</sup>C NMR (100.6 MHz, CDCl<sub>3</sub>) 13.9 (CH<sub>3</sub>CH<sub>2</sub>), 22.3 (CH<sub>3</sub>CH<sub>2</sub>CH<sub>2</sub>), 22.9 (CH<sub>3</sub>CO), 25.1 (CH<sub>2</sub>CH<sub>2</sub>CO), 28.9 (SCH<sub>2</sub>), 31.4 (CH<sub>3</sub>CH<sub>2</sub>CH<sub>2</sub>), 36.3 (CH<sub>2</sub>CH<sub>2</sub>CO), 38.6 (NHCH<sub>2</sub>), 61.3 (CHCH<sub>2</sub>O), 62.7 (CHCH<sub>2</sub>OH), 171.77 (NHCOCH<sub>3</sub>), 174.19 (CH<sub>2</sub>CONH), 200.08 (CHCOS); LRMS-ESI (*m/z*) 305.2 ([M + H]<sup>+</sup>, 100%), 327.2 [M + Na]<sup>+</sup>, 343.2 [M + K]<sup>+</sup>, 631.4 [2M + Na]<sup>+</sup>; HRMS-ESI (*m/z*) [M + H]<sup>+</sup> calcd for C<sub>13</sub>H<sub>25</sub>N<sub>2</sub>O<sub>4</sub>S, 305.1535. Found, 305.1543. IR (neat): ν 3292 (OH), 2930 (CH), 1656 (C=O), 1540 (NH, amide) cm<sup>–1</sup>. [α]<sub>D</sub> = –26.2° (*c* = 1.0, CHCl<sub>3</sub>).

**Nα-Pentanoyl-L-serine N-Acetylcysteamine Thioester (4).** L-Ser-NAC·HCl **2** (300 mg, 1.24 mmol) was acylated with pentanoyl chloride (150 μL, 1.24 mmol) to give product **4** (260 mg, 72% yield) as a clear oil. *R*<sub>f</sub> 0.15 (5% CH<sub>3</sub>OH in EtOAc); <sup>1</sup>H NMR (400 MHz, CDCl<sub>3</sub>) 0.90 (3H, t, *J* = 7.3 Hz, CH<sub>3</sub>CH<sub>2</sub>), 1.31–1.40 (2H, m, CH<sub>3</sub>CH<sub>2</sub>), 1.59–1.67 (2H, m, CH<sub>3</sub>CH<sub>2</sub>CH<sub>2</sub>), 1.94 (3H, s, CH<sub>3</sub>CO), 2.27–2.30 (2H, m, CH<sub>2</sub>CH<sub>2</sub>CO), 2.92–3.04 (2H, m, SCH<sub>2</sub>), 3.32–3.47 (2H, m, NHCH<sub>2</sub>), 3.75 (1H, dd, *J* = 3.6, 11.6 Hz, CHCH<sub>a</sub>H<sub>b</sub>O), 4.07 (1H, dd, *J* = 3.3, 11.6 Hz, CHCH<sub>a</sub>H<sub>b</sub>O), 4.57–4.61 (1H, m, CHCH<sub>2</sub>), 6.81 (1H, brs, CH<sub>2</sub>NHCO), 7.15 (1H, d, *J* = 7.9, CHNHCO); <sup>13</sup>C NMR (100.6 MHz, CDCl<sub>3</sub>) δ 13.7 (CH<sub>3</sub>CH<sub>2</sub>), 22.3 (CH<sub>3</sub>CH<sub>2</sub>), 23.0 (CH<sub>3</sub>CO), 27.5 (CH<sub>3</sub>CH<sub>2</sub>CH<sub>2</sub>), 28.9 (SCH<sub>2</sub>), 36.1 (CH<sub>2</sub>CH<sub>2</sub>CO), 38.6 (NHCH<sub>2</sub>), 61.2 (CHCH<sub>2</sub>O), 62.6 (CHCH<sub>2</sub>O), 171.7 (CH<sub>3</sub>CONH), 174.2 (CH<sub>2</sub>CONH), 200.0 (SCOH); LRMS-ESI (*m/z*) 291.0 [M + H]<sup>+</sup>, 313.0 [M + Na]<sup>+</sup>, 581.1 [2M + H]<sup>+</sup>, 603.0 [2M + Na]<sup>+</sup>, 619.0 [2M + K]<sup>+</sup>; HRMS-ESI (*m/z*) [M + Na]<sup>+</sup> calcd for C<sub>12</sub>H<sub>22</sub>N<sub>2</sub>NaO<sub>4</sub>S, 313.1192. Found, 313.1186. [α]<sub>D</sub> = –34.1° (*c* = 1.0, CHCl<sub>3</sub>). IR (neat): ν 3288 (OH), 2931 (CH), 1656 (CO), 1542 (NH, amide) cm<sup>–1</sup>.

**Nα-Heptanoyl-L-serine N-Acetylcysteamine Thioester (6).** L-Ser-SNAC·HCl **3** (220 mg, 0.9 mmol) was similarly acylated with heptanoyl chloride (140 μL, 0.9 mmol) to give product **6** (193 mg, 67%) as a clear oil. *R*<sub>f</sub> = 0.2 (5% CH<sub>3</sub>OH in EtOAc); <sup>1</sup>H NMR (400 MHz, CDCl<sub>3</sub>) δ 0.86 (3H, t, *J* = 6.7 Hz, CH<sub>3</sub>CH<sub>2</sub>), 1.28 (6H, m, CH<sub>3</sub>CH<sub>2</sub>CH<sub>2</sub>CH<sub>2</sub>), 1.66 (2H, m, CH<sub>2</sub>CH<sub>2</sub>CO), 1.97 (3H, s, CH<sub>3</sub>CO), 2.28 (2H, t, *J* = 7.6 Hz, CH<sub>2</sub>CH<sub>2</sub>CO), 2.88–3.08 (2H, m, SCH<sub>2</sub>), 3.38–3.63 (2H, m, NHCH<sub>2</sub>), 3.74 (1H, dd, *J* = 3.7 Hz, 11.7 Hz, CHCH<sub>a</sub>H<sub>b</sub>O), 4.14 (1H, dd, *J* = 2.1, 11.7 Hz, CHCH<sub>a</sub>H<sub>b</sub>O), 4.62 (1H, m, CHCH<sub>2</sub>),

5.94 (1H, br s, NHCH<sub>2</sub>), 6.60 (1H, d, *J* = 7.66 Hz, NHCH); <sup>13</sup>C NMR (100.6 MHz, CDCl<sub>3</sub>) δ 14.3 (C7), 22.7 (C6), 23.4 (CH<sub>3</sub>CO), 25.6 (C3), 29.2 (C5), 29.5 (SCH<sub>2</sub>), 31.7 (C4), 36.7 (C2), 38.7 (NHCH<sub>2</sub>), 61.4 (CHCH<sub>2</sub>O), 63.2 (CHCH<sub>2</sub>O), 171.9 (CH<sub>3</sub>CONH), 174.2 (CH<sub>2</sub>CONH), 200.3 (SCOH); LRMS-ESI (*m/z*) 319.1 [M + H]<sup>+</sup>, 341.0 [M + Na]<sup>+</sup>, 637.1 [2M + H]<sup>+</sup>, 659.1 [2M + Na]<sup>+</sup>; HRMS-ESI (*m/z*) [α]<sub>D</sub><sup>32</sup> = –34.4° (*c* = 1.0, CHCl<sub>3</sub>). IR (neat): ν 3289 (OH), 2926 (CH), 1646 (CO), 1530 (NH, amide) cm<sup>–1</sup>.

**Nα-Decanoyl-L-serine N-Acetylcysteamine Thioester (5).** To N-hydroxy succinimide (690 mg, 6.0 mmol) and triethylamine (708 mg, 7.0 mmol) in THF (10 mL) was added decanoyl chloride (572 mg, 3.0 mmol) dropwise over 5 min, and it was left to stir for 3 h at room temperature. The solvent was evaporated under reduced pressure, and the residue was partitioned between water (40 mL) and DCM (3 × 30 mL). The organic extracts were dried over MgSO<sub>4</sub> and evaporated. THF (20 mL) was added to the residue, followed by triethylamine (405 mg, 4.0 mmol) and L-Ser-SNAC·HCl **2** (485 mg, 2.0 mmol). The mixture was left to stir for 15 h at room temperature, evaporated, and water (40 mL) was added. The mixture was then extracted with CH<sub>2</sub>Cl<sub>2</sub> (3 × 50 mL). The organic extracts were dried (MgSO<sub>4</sub>), evaporated, and purified by column chromatography eluting with 5% MeOH in EtOAc followed by trituration with *n*-hexane to give the desired product (560 mg, 76%) as a white powder. *R*<sub>f</sub> = 0.4 (10% CH<sub>3</sub>OH in EtOAc); mp 68–71 °C, <sup>1</sup>H NMR (300 MHz, CDCl<sub>3</sub>) 0.85 (3H, t, *J* = 6.8 Hz, CH<sub>3</sub>CH<sub>2</sub>), 1.24 (12H, m, CH<sub>3</sub>(CH<sub>2</sub>)<sub>6</sub>), 1.64 (2H, m, CH<sub>2</sub>CH<sub>2</sub>CO), 1.94 (3H, s, CH<sub>3</sub>CO), 2.27 (2H, t, *J* = 7.6 Hz, CH<sub>2</sub>CH<sub>2</sub>CO), 2.88–3.07 (2H, m, SCH<sub>2</sub>), 3.32–3.59 (2H, m, NHCH<sub>2</sub>), 3.74 (2H, m, CHCH<sub>a</sub>H<sub>b</sub>O and OH), 4.13 (1H, m, CHCH<sub>a</sub>H<sub>b</sub>O), 4.61 (1H, m, CHCH<sub>2</sub>), 6.11 (1H, t, *J* = 5.9 Hz, CH<sub>2</sub>NHCO), 6.72 (1H, d, *J* = 8.0 Hz, CHNHCO); <sup>13</sup>C NMR (75.4 MHz, CDCl<sub>3</sub>) δ 14.3 (C10), 22.9 (C9), 23.4 (CH<sub>3</sub>CO), 25.7 (C8), 29.4 (SCH<sub>2</sub>), 29.5 (C7), 29.6 (C6), 29.7 (C5), 32.1 (C3 & C4), 36.7 (C2), 38.5 (NHCH<sub>2</sub>), 61.3 (CHCH<sub>2</sub>O), 63.3 (CHCH<sub>2</sub>O), 171.7 (CH<sub>3</sub>CONH), 174.0 (CH<sub>2</sub>CONH), 200.3 (SCOH); LRMS-ESI (*m/z*) 361.2 [M + H]<sup>+</sup>, 383.2 [M + Na]<sup>+</sup>, 721.4 [2M + H]<sup>+</sup>, 743.4 [2M + Na]<sup>+</sup>; HRMS-ESI (*m/z*) [M + H]<sup>+</sup> calcd for C<sub>17</sub>H<sub>33</sub>N<sub>2</sub>O<sub>4</sub>S, 361.2156. Found, 361.2163. [α]<sub>D</sub> = –34.6° (*c* = 1.0, CHCl<sub>3</sub>). IR (neat): ν 3290 (OH), 2925 (CH), 2854 (CH), 1654 (CO), 1543 (NH, amide) cm<sup>–1</sup>. Anal. Calcd for C<sub>17</sub>H<sub>32</sub>N<sub>2</sub>O<sub>4</sub>S: C, 56.64; H, 8.95; N, 7.77; S, 8.89. Found: C, 56.55; H, 8.99; N, 7.51; S, 8.62.

**Deletion of *hxcO* from *S. coelicolor* MT1110.** A “double crossover” gene replacement strategy<sup>1a,10</sup> was used to delete *hxcO* (SCO3247) from the chromosome of the *S. coelicolor* MT1110 parent strain. Two fragments A and B that flank the chromosomal sequence to be deleted were ligated into *E. coli* plasmid pMT3000 and cloned using host strain *E. coli* XL1 BLUE. The upstream fragment A was generated by PCR using 2E5 cosmid DNA<sup>28</sup> as the template with the forward primer (5′-CAA CTG CAG CCA CGT GCC CCG ATA ACG, encompassing the nucleotide coordinates 3602414–3602431 and a *Pst*I site) and reverse primer (5′-CGC CTC GAG CGC GAT CTG GTG CGA GA encompassing the nucleotide coordinates 3600545–3600561 and a *Xho*I site). The downstream fragment B was similarly generated using the same cosmid as the template with the forward primer (5′-CTG CTC GAG TGC TGC GTG CTG GAA CA, encompassing the nucleotide coordinates 3599324–3599338 and a *Xho*I site) and reverse primer (5′-ACC GAA TTC CCG GTG GAT CGT GTA, encompassing the nucleotide coordinates 3597650–3597664 and a *Eco*R1 site). The cloned deletion fragment A+B was extracted from the plasmid by restriction digestion, with *Bgl*III, purified, and then used in a ligation reaction with *Bam*HI restriction digested pMAH vector<sup>18</sup> (via a *Bam*HI: *Bgl*III ligation). The ligation mix was in turn used to transform *E. coli*

- (28) Chong, P. P.; Podmore, S. M.; Kieser, H. M.; Redenbach, M.; Turgay, K.; Marahiel, M.; Hopwood, D. A.; Smith, C. P. *Microbiology* **1998**, *144*, 193–199.  
 (29) Redenbach, M.; Kieser, H. M.; Denapaite, D.; Eicher, A.; Cullum, J.; Kinashi, H.; Hopwood, D. A. *Mol. Microbiol.* **1996**, *21*, 77–96.  
 (30) Lakey, J. H.; Lea, E. J. A.; Rudd, B. A. M.; Wright, H. M.; Hopwood, D. A. *J. Gen. Microbiol.* **1983**, *129*, 3565–3573.

XL1 BLUE competent cells from which the pMAH vector containing the deletion construct was re-isolated and similarly used to transform *E. coli* strain ET12567. The resulting nonmethylated plasmid was then used to transform protoplasts of *S. coelicolor* MT1110. Spores were prepared from hygromycin resistant colonies, and Hyg sensitive colonies (putative deletants) were identified following two rounds of nonselective subculturing. Total DNA extraction<sup>17</sup> followed by PCR-analysis, sequencing, and Southern blots confirmed the loss of 1206 bp from within *hxcO* (see Supporting Information).

**Deletion of *hcmO* from *S. coelicolor* MT1110.** The *hcmO* (SCO3245) gene was deleted from the chromosome of the *S. coelicolor* MT1110 parent strain in an identical fashion. The upstream fragment A in this case was generated by PCR using 2E5 cosmid DNA<sup>28</sup> as the template with the forward primer (5'- TTC TGC AGT TCG GCG GTG ACA ACA, encompassing the nucleotide coordinates 3599617–3599632 and aa *Pst*I site underlined) and reverse primer (5'- CTA CTC GAG G CC CCA GCG TTC CAG AA encompassing the nucleotide coordinates 3597794–3597810 and a *Xho*I site). The downstream fragment B was similarly generated using the same cosmid as the template with the forward primer (5'- CCG CTC GAG CGC AGG CCG CAC AC, encompassing the nucleotide coordinates 3596871–3596884 and a *Xho*I site) and reverse primer (5'- CGA GGC GTG AAT TCC GGT ACG CAT GAT GTC T, encompassing the nucleotide coordinates 3595784–3595800 and a *Eco*R1 site). Total DNA extraction<sup>17</sup> from the  $\Delta hcmO$  mutant strains followed by PCR-analysis, sequencing, and Southern blots confirmed the loss of 909 bp from within *hxcO* (see Supporting Information).

**CdaPS1 PCP Domain Ser1122→Ala Mutation.** A 1523 bp fragment encompassing the module 1 PCP domain of *cdaPS1* was obtained by PCR amplification from the cosmid E63<sup>29</sup> with the following forward primer (5'-CGC GCT GGA TCC ACG ACG GC, encompassing the nucleotide coordinates 3545918–3545938 and a *Bam*HI site) and reverse primer (5'-AGT GGG CAA GCT TCC GGG CGC, encompassing the nucleotide coordinates 3547435–3547456 and a *Hind*III site). The PCR product was then restricted with *Bam*HI and *Hind*III, ligated into pGEM-11Zf(+), and used to transform *E. coli* XL1-Blue. The resulting plasmid was isolated, and the Stratagene site-directed mutagenesis (QuikChange) approach was used to obtain the module 1 PCP-domain single-point mutation (Ser1122→Ala) using a forward mutagenic oligonucleotide (5'- GC GGC CAC GCG CTG CTC, encompassing the nucleotide coordinates 3546689–3546705 with the TCG (Ser) to GCG (Ala) codon change underlined) and a complementary reverse mutagenic oligonucleotide. The mutated DNA fragment was extracted from the plasmid by restriction digestion with *Bam*HI and *Hind*III, purified, and ligated into the *Bam*HI and *Hind*III digested pMAH vector.<sup>18</sup> Transformation of *E. coli* XL1-Blue and demethylation in *E. coli* ET12567 gave the non-methylated plasmid containing the point mutation, which was used to transform *S. coelicolor* MT1110 protoplasts. Double crossover mutants were isolated as described above, and the desired mutation was confirmed by sequencing the genomic DNA (see Supporting Information).

**Cultivation of *S. coelicolor*, and Extraction and Analysis of CDA.** MT1110 parental and mutant strains were seeded on R5<sup>17</sup> plates and used to inoculate SV2 liquid media.<sup>1a</sup> This was then incubated for 5 days at 28 °C with shaking (180 rpm). Alternatively, MT1110 parental and mutant strains were grown on R5 solid media for 7 days at 28 °C. The supernatants from liquid culture, or the freeze–thaw exudate from solid media, were then adjusted to pH 2.0 and extracted with Varian C-18 Bond Elute SPE cartridges, which were washed with water then 30–50% aqueous methanol. The CDA extracts were then eluted with 100% aqueous methanol, evaporated under reduced pressure, and analyzed by LC–MS.<sup>10a</sup>

**Purification of CDAs.** CDA extracts were purified by semipreparative reversed phase HPLC: Phenomenex C-18 10 mm, 250 × 21.2 mm and 5 mm, 250 × 10 mm columns. Solvent A was H<sub>2</sub>O with 0.1% HCO<sub>2</sub>H, and solvent B was acetonitrile with 0.1% HCO<sub>2</sub>H. The flow rate was 5 mL min<sup>-1</sup> starting with 0% B and 100% A, increasing to 100% B over 30 min, and then held for a further 5 min. Separate 1 min fractions were collected over the program. Fractions were analyzed by LC–MS, and those fractions containing CDAs were pooled and then purified by further semipreparative reversed phase HPLC (as above) except the starting gradient was 70% A and 30% B, which increased to 40% B over 35 min with a further increase to 60% B in the following 5 min.

**Mass Spectrometric Analyses of Purified CDAs.** HRMS, MS–MS, and MS<sup>n</sup> analysis was performed on a 9.4T Bruker Daltonics Apex III FT-ICR mass spectrometer using direct infusion electrospray with CDA peptides (10 pmol  $\mu$ L<sup>-1</sup>). The gas-phase precursor ions were preisolated in the ICR cell by applying a correlated RF-sweep and cooled using argon gas. The precursor ions were then fragmented by infrared multiphoton dissociation (IRMPD) using a Synrad J48.2W CO<sub>2</sub> laser (10.6 mm, 35 W), 0.25 s irradiation at 12.5% PWM, and the resulting product ion spectrum was recorded. In addition, MS–MS and MS<sup>n</sup> analysis was carried out on a Bruker Esquire 3000+, ion trap LC–MS, equipped with an electrospray ionization source run in positive mode (scanning from 100 to 1500 *m/z*). Gradient elution was carried out using a reversed phase LC Packings C-18 150 × 0.75 mm 3  $\mu$ m Dinex column. Solvent A was H<sub>2</sub>O with 0.1% HCO<sub>2</sub>H. Solvent B was acetonitrile with 5% H<sub>2</sub>O and 0.1% HCO<sub>2</sub>H. The flow rate was 0.25 mL min<sup>-1</sup> with a gradient of 95% A and 5% B, increasing to 40% B over 2 min, and then held for 10 min. The gradient was then increased to 100% B over the next 13 min and then held for a further 17 min.

**CDA Bioassays.** Well-based plate bioassays were carried out on Oxoid nutrient agar plates as described previously<sup>10b</sup> using *Micrococcus luteus* as an indicator strain in the presence or absence of CaNO<sub>3</sub> (16 mM). CDA samples ranging from 2 to 20  $\mu$ g in 100  $\mu$ L total volume were added to 5 mm wells, bored into the agar, and incubated at 30 °C for 1–3 days.

**Feeding *N*-Acyl-serinyl NAC Derivatives to MT1110- $\Delta pcp_1$ .** *N*-acyl-serinyl NAC thioesters **3**, **4**, and **6** were dissolved in deionized water, and **5** was dissolved in the minimum amount of 50% aqueous ethanol.<sup>23</sup> These solutions were then fed at the following increasing total concentrations (0.1, 0.2, 0.3, 0.4, 0.5, 1.7, 2.3, 2.9, 3.5, and 4.0 mg mL<sup>-1</sup>) to *S. coelicolor* MT1110- $\Delta pcp_1$  grown for 2 days in SV2 liquid medium. The cultures were grown for a further 4 days at 28 °C and 180 rpm, worked up, and analyzed as described above.

**Acknowledgment.** This work was supported by the BBSRC through research grants 36/B12126 and BB/C503662, and through a studentship to A.P. Biotica is also acknowledged for CASE awards and support to A.P. We also thank Prof. Simon Gaskell and Dr. Stephen Wong in the Michael Barber Centre for Mass Spectrometry (Manchester) for assistance with FTICR-MS. We thank Dr. Claire Milne (Manchester) for preliminary results and Drs. Fiona Flett (Manchester) and Christoph Beckmann (Biotica) for helpful advice and discussion.

**Supporting Information Available:** Additional data, figures, and experimental details. This material is available free of charge via the Internet at <http://pubs.acs.org>.

JA074331O